

H4-SMR 1012 - 12

AUTUMN COLLEGE ON PLASMA PHYSICS

13 October - 7 November 1997

CONTROL OF CHAOS IN DUSTY PLASMAS

B. BUTI

National Physical Laboratory, New Delhi, India

These are lecture notes, intended for distribution to participants.

CONTROL of CHAOS in DUSTY PLASMAS

B. Buti
National Physical Laboratory
New Delhi 110012, India

Abstract

Dusty plasmas, besides electrons and protons, contain very massive charged dust grains with very high charges. By means of Poincare map analysis, we show that even a small fraction of these charged dust grains can eliminate the chaos in Alfvénic systems which are chaotic in the absence of dust particles.

Dusty plasmas are prevalent in many cosmic as well as space plasmas such as planetary rings, planetary magnetospheres, cometary environment, interstellar medium etc. [1-4]. Here we would like to distinguish between plasmas with a few dust grains and plasma where dust grains, satisfying the condition $N_d \lambda_d^3 \gg 1$ (N_d being the density of charged dust grains and λ_d the Debye length), form the third constituent of plasma. Only the latter ones we would define as dusty plasmas; such plasmas, one encounters in process plasma e.g., chip manufacture besides the cosmic plasmas.

The question of controlling chaos, in dissipative systems, was first discussed by Ott et al. [5]. The chaotic attractors, associated with dissipative dynamical systems, usually have a dense set of unstable periodic orbits embedded in them. Ott et al. suggested that one should first determine some of the low -period unstable periodic orbits embedded in the chaotic attractor. Then choose one, out of these unstable orbits, which yields improved performance when a small change is made in a parameter. Finally adjust the small parameter in such a way that the unstable periodic orbit is stabilized.

In this paper, we suggest an alternative way of controlling chaos in nondissipative systems e.g., a plasma which can be described as a driven Hamiltonian system.

PHYS. LETT. A (IN PRESS)

As a specific example, we have chosen magnetoplasma where nonlinear Alfvén waves can exist. These large amplitude Alfvén waves, in fact, have been observed in a variety of plasmas e.g., interplanetary medium, planetary bow shocks, cometary environment etc. [6,7,8]. Nonlinear evolution of these waves, in a 2-species plasma, has been extensively studied by Rogister [9], Mjølhus and Wyller [10], Kennel et al. [11], Buti [12] and Spangler [13]. The solitary Alfvén waves, investigated by these authors, have been shown to become chaotic in the presence of a driver by Hada et al. [14], Buti [15] and Nocera and Buti [16]. Buti [17] extended these investigations to multi-species plasmas and showed that even a small fraction of heavy ions like helium can drastically reduce the chaos simply due to inertial stabilization effect of α - particles. In the present paper, we have further extended these investigations to dusty plasmas to explore the effect of real massive heavily charged dust grains on chaotic Alfvénic systems. Interestingly, we find that because of dust grains, chaos is not only reduced but it simply disappears even with dust grain densities as small as 10^{-8} of the proton density.

Nonlinear Alfvén waves in dusty plasmas are governed by [18],

$$\frac{\partial \vec{B}_\perp}{\partial t} + \alpha \frac{\partial}{\partial x} (\vec{B}_\perp | \vec{B}_\perp |^2) + \mu \left(\hat{e}_x \times \frac{\partial^2 \vec{B}_\perp}{\partial x^2} \right) + \delta \vec{B}_\perp = 0, \quad (1)$$

where $\vec{B}_\perp = (B_y, B_z)$ represents normalized magnetic field fluctuations in a plane transverse to the direction of propagation which is taken along x - axis. Eq. (1) is same as the one for multispecies plasmas [17, 19] except for the additional (last term) source term which is due to charge fluctuations of dust grains. The co-efficients α, μ and δ for cold plasmas are given by:

$$\alpha = \frac{1}{4A}, \quad (2a)$$

$$A = \sum_s \rho_s (V - U_s), \quad (2b)$$

$$\mu = \frac{1}{2A} \sum_s \frac{\rho_s (V - U_s)^3}{\Omega_s}, \quad (2c)$$

$$\delta = \frac{1}{2A} \sum_s \sum_r (\rho_s \gamma_{sr} - \rho_r \gamma_{rs}) U_r, \quad (2d)$$

where ρ_s is the mass density, Ω_s is the cyclotron frequency and U is the drift velocity in equilibrium. Note that in the absence of any equilibrium drift i.e., for $U_s = 0$, the source term vanishes; in this case V reduces to the Alfvén speed ($V_A = (B_o / (4\pi \rho))^{1/2}$).

For 3- species plasma with electrons, protons and heavy dust grains, these coefficients are simply given by,

$$\alpha = \frac{1}{4} \left(1 + \frac{\rho_d}{(\rho_e + \rho_p)} \right)^{-1/2}, \quad (3a)$$

$$\mu = \frac{1}{2A} \left(1 + \frac{\rho_d}{(\rho_e + \rho_p)} \right)^{-2} \left(1 + \frac{\rho_d \Omega_p}{\rho_p \Omega_d} + \frac{\rho_e \Omega_p}{\rho_p \Omega_e} \right), \quad (3b)$$

$$\delta = 0. \quad (3c)$$

In Eqs.(3), the subscripts e, p and d represent electrons, protons and dust grains respectively. For 2-species plasma i.e., for $N_d = 0$, note that $V = A = 1$, $\alpha = 1/4$ and $\mu = 1/2$. In writing Eqs.(3), we have made use of the charge neutrality condition, i.e., $(N_e + Z_d N_d) = N_p$. In the presence of an external driver, Eq. (1) gets modified; the source term $S(\vec{B}_\perp, x, t)$ appears on the right hand side of Eq. (1) [14]. For a plane circularly polarised driver i.e., for $S = a \exp(i k \xi)$, Eq. (1) can be written in terms of the Hamiltonian of the system [17], namely,

$$\frac{dB_y}{d\xi} = -\frac{\partial H}{\partial B_x} - \frac{a}{2\mu} \cos \theta, \quad (4a)$$

$$\frac{dB_x}{d\xi} = \frac{\partial H}{\partial B_y} - \frac{a}{2\mu} \sin \theta, \quad (4b)$$

$$\frac{\partial \theta}{\partial \xi} = \Omega, \quad (4c)$$

where $\xi = (x - V t) / 2$, a and Ω as the amplitude and the frequency of the driver and H the Hamiltonian which is given by,

$$H(\vec{B}) = \frac{1}{2} \frac{\alpha}{\mu} (B^2 - 1)^2 - \frac{\Lambda}{2} (\vec{B} - \hat{e}_y)^2, \quad (5)$$

with

$$\Lambda = \frac{2}{\mu} \left(\frac{V}{b^2} - \alpha \right) \quad (6)$$

and b as the asymptotic value of B .

As mentioned earlier, dusty plasmas are observed in nebulas, planetary rings, planetary magnetospheres and cometary environment. We have solved Eq. (1) numerically for the case of rings of Saturn and for the cometary cases. In these systems, dust grain size is typically a few microns and dust mass is on the order of $10^{12} m_p$. The dust grains carry very high charges; typically $Z_d \sim (10^3 - 10^4)e$ [4]. However the

dust number densities could be as low as $(10^{-8} - 10^{-6}) N_p$. For these parameters α and μ simply reduce to,

$$\alpha \simeq \frac{1}{4} \left(\frac{\rho_p}{\rho_d} \right)^{1/2} \quad (7)$$

and

$$\mu \simeq \frac{1}{2} \frac{\rho_p \Omega_p}{\rho_d \Omega_d} = \frac{1}{2} \frac{N_p}{N_d Z_d}. \quad (8)$$

Thus it is apparent that the crucial parameters, governing the nonlinear dynamics, are the mass density and the charge of the dust grains.

The results of numerical computations are shown in Figs.1 – 9. The points on Poincare maps correspond to the orbits satisfying the condition $\theta = 2n\pi$; n being a positive integer. Fig.1 shows that even for a weak driver corresponding to $a = 0.3$, or even for smaller a (not shown here), Alfvén waves in a 2 - species plasma (without dust grains) become chaotic. However in dusty plasmas as shown in Figs.2 – 4 and Figs.6 – 8 for cometary plasmas and in Figs.5 and 9 for Saturn rings, Poincare maps do not show any chaos; one gets only periodic orbits even for strong drivers with amplitudes which are order of magnitude larger compared to the one for 2 - species plasma. For Figs. 2,3,4 and 5, the driver is a right hand polarised driver and the results shown correspond to a number of initial conditions. However, for Figs. 6,7,8 and 9, we have taken the left hand driver and orbits shown are for a single initial condition. For other initial conditions considered in Figs.2–5 also, we get (not shown here) similar periodic orbits. From these results (Figs.2 – 9), we can straightaway conclude that the chaos in Alfvénic systems simply disappears due to the presence of massive dust grains.

Here we have confined ourselves to dusty plasmas but this technique can be fruitfully used for controlling chaos in other plasmas e.g., fusion plasmas also. All that one has to do is to introduce a small fraction of heavy ions, like an impurity, in the region which is found to be chaotic. These results will be published in a forthcoming paper.

In the present paper, we have presented the results for nonstreaming plasmas. For streaming plasmas i.e., for $\delta \neq 0$, work is in progress and will be reported elsewhere.

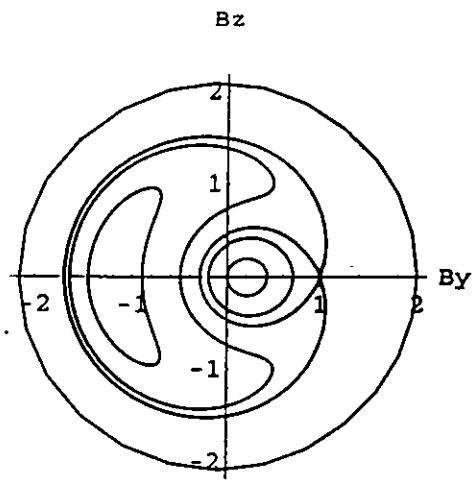
I would like to express my gratitude to E.Ott, D.A.Mendis and T.G.Northrop for very helpful discussions.

REFERENCES

1. L. Spitzer Jr. *Physical Processes in Interstellar Medium*, Wiley, New York. 1978.
2. C.K.Goertz, *Rev. Geophys.* 27 (1989) 271.
3. T.G.Northrop, *Physica Scripta*, 45 (1992) 475.
4. D.A. Mendis and M. Rosenberg, *Ann. Rev. Astron. Astrophys.* 32 (1994) 419.
5. E.Ott, C. Grebogi and J.A.York, *Phys. Rev. Lett.* 64 (1990) 1196.
6. B.T. Tsurutani and E.J. Smith, *Geophys. Res. Lett.*13 (1986) 259.
7. F.L. Scarf, F.V. Coroniti, C.F. Kennel, D.A. Gurnett and E.J. Smith, *Science* 232 (1986) 382.
8. L.F. Burlaga, *Rev. Geophys. Space Phys.* 21 (1983) 363.
9. A.Rogister, *Phys. Fluids*, 14 (1971) 2733.
10. E.Mjolhus and J.Wyller, *Jou. Plasma Phys.* 40 (1988) 299; *Physica Scripta*, 33 (1986) 442.
11. C.F. Kennel, B. Buti, T. Hada and R. Pellat, *Phys. Fluids* 31 (1988) 1949.
12. B. Buti, *Cometary and Solar Plasma Physics*, Ed. B. Buti, World Scientific, Singapore (1988) 221.
13. S.R.Spangler, *Phys. Fluids*, B1 (1989) 1738; B2 (1990) 407.
14. T. Hada, C.F. Kennel, B. Buti and E. Mjolhus, *Phys. fluids* B2 (1990) 2581.
15. B. Buti, *Solar and Planetary Plasma Physics*, Ed. B. Buti, World Scientific, Singapore (1990) 92.
16. L.Nocera and B.Butu, *Physica Scripta* T63 (1996) 186.
17. B. Buti, *Jou. Geophys. Res.* 97 (1992) 4229.
18. F. Verheest and P.Meuris, *Phys.Lett.* 210A (1996) 198.
19. F. Verheest and B. Buti, *Jou. Plasma Phys.* 47 (1992) 15.

FIGURE CAPTIONS

- Fig. 1 Poincare maps for driven Hamiltonian system with right hand driver with $\Omega = -2$ and $V/b^2 = 5/16$ for various initial conditions but without the dust grains.
- Fig. 2 Same as Fig.1 but with the dust grains with $N_d/N_p = 1.7 \times 10^{-4}$, $Z_d = 10^3$, $m_d/m_p = 10^{12}$.
- Fig. 3 Same as Fig.2 but with $N_d/N_p = 4 \times 10^{-6}$ and $Z_d = 10^4$.
- Fig. 4 Same as Fig.2 but with $N_d/N_p = 10^{-6}$ and $Z_d = 4 \times 10^3$.
- Fig. 5 Same as Fig.2 but for Saturn Rings with $N_d/N_p = 4 \times 10^{-8}$ and $Z_d = 10^4$.
- Fig. 6 Same as Fig.2 but with left hand driver with $\Omega = 2$ and for single initial condition with $(B_y, B_z) = (1.00001, 0)$ and the amplitude of the driver $a = 0, 0.8, 10$ and 25 .
- Fig. 7 Same as Fig.6 but with $N_d/N_p = 4 \times 10^{-6}$ and $Z_d = 10^4$, and $a = 0, 0.8, 10$ and 50 .
- Fig. 8 Same as Fig.6 but with $N_d/N_p = 10^{-6}$ and $Z_d = 4 \times 10^3$, and $a = 0, 0.8, 10$ and 50 .
- Fig. 9 Same as Fig.6 but for Saturn Rings with $N_d/N_p = 4 \times 10^{-8}$ and $Z_d = 10^4$ and the amplitude of the driver $a = 0, 0.8, 10$ and 25 .



$$a = 0.3$$

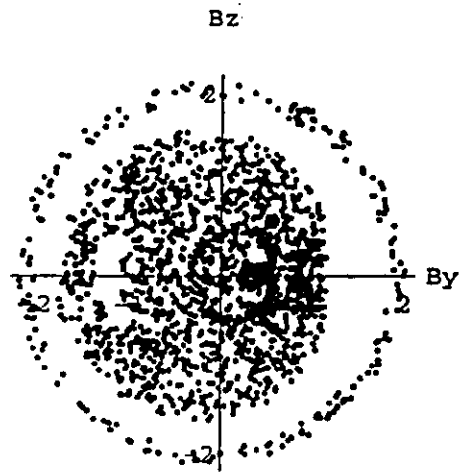
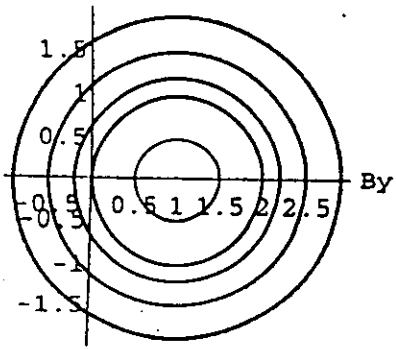


Fig. 1

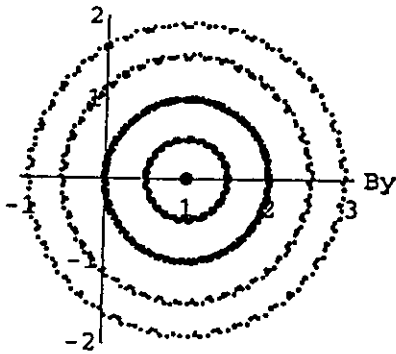
$$a = 0$$

Bz



$$a = 0.3$$

Bz



$$a = 1.8$$

Bz

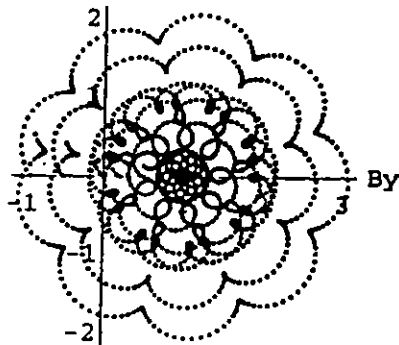
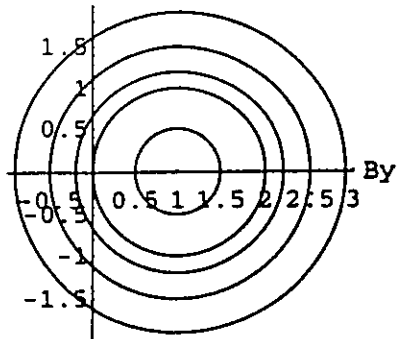


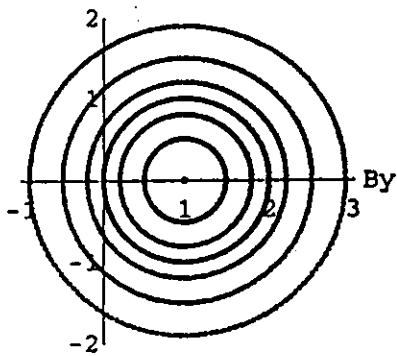
Fig 2

Bz



$a = 0.3$

Bz



$a = 7.5$

Bz

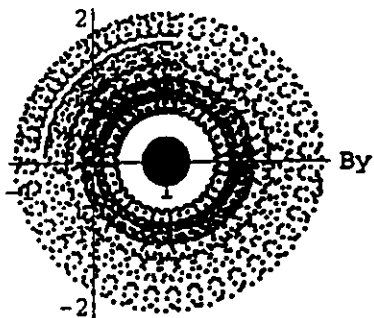
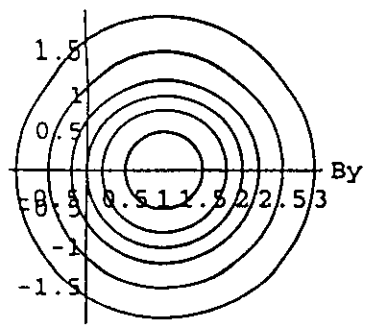


Fig. 3

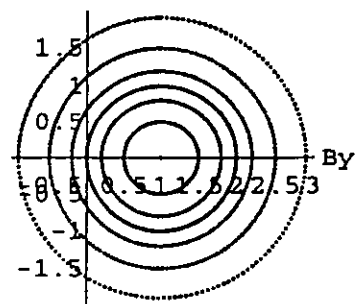
$a = 0$

Bz



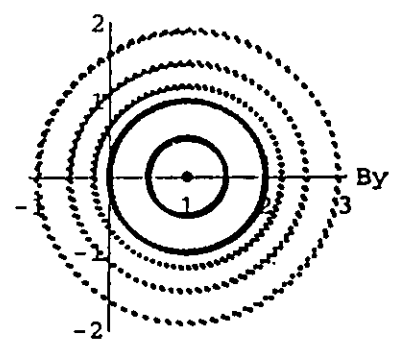
$a = 0.3$

Bz



$a = 10$

Bz



$a = 25$

Bz

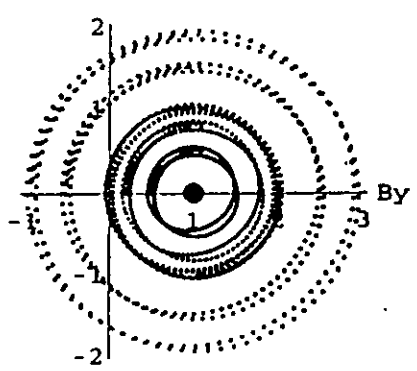
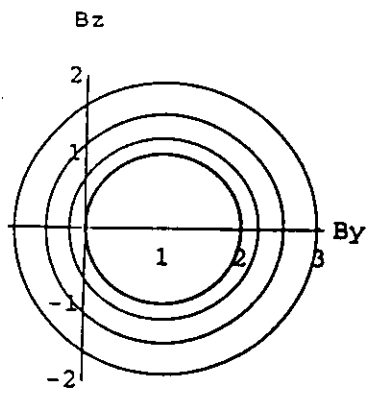
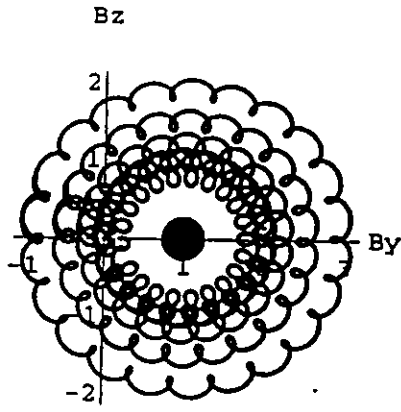


Fig. 4



$a = 10$



$a = 25$

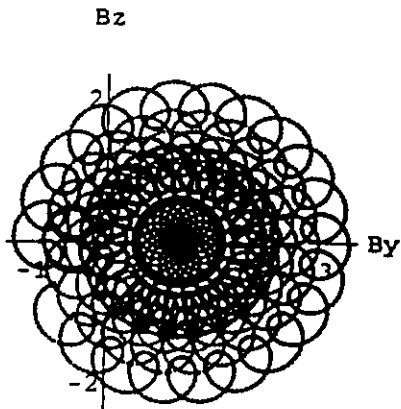
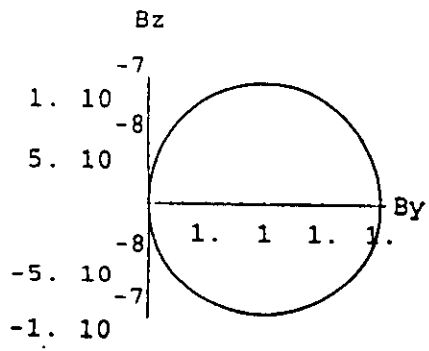
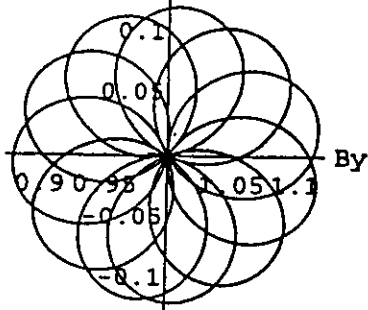


Fig 5



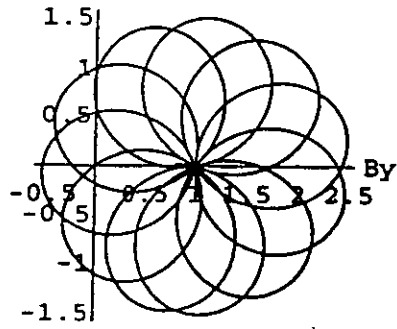
$a = 0.8$

Bz



$a = 10$

Bz



$a = 25$

Bz

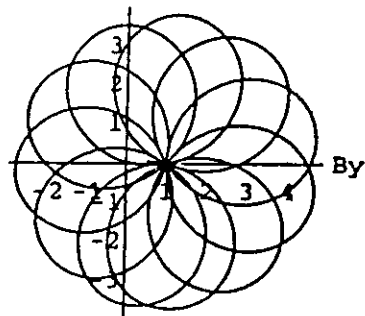
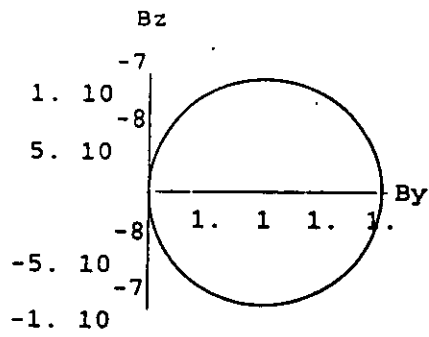
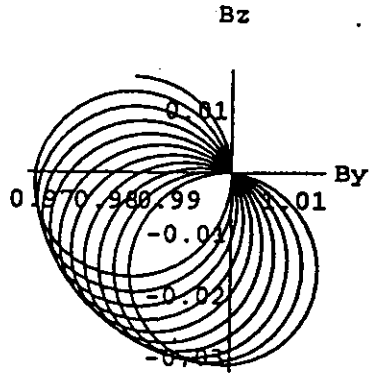


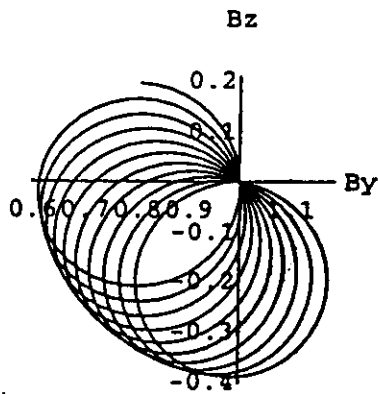
Fig. 6



$a = 0.8$



$a = 10$



$a = 50$

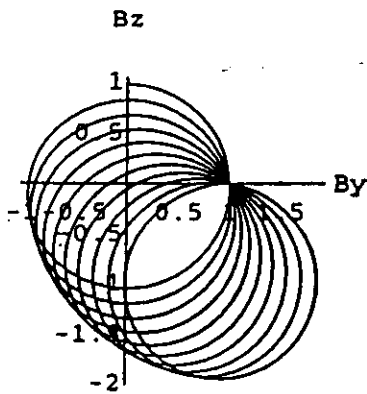
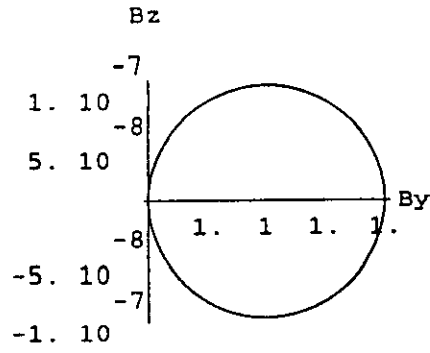
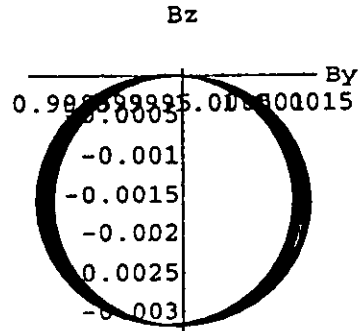


Fig. 7

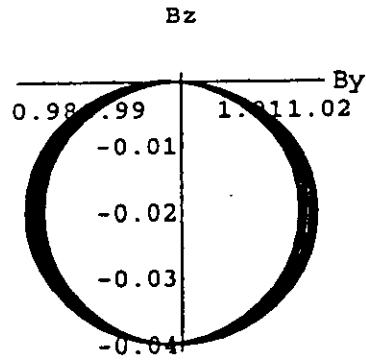
a = 0



a = 0.8



a = 10



a = 50

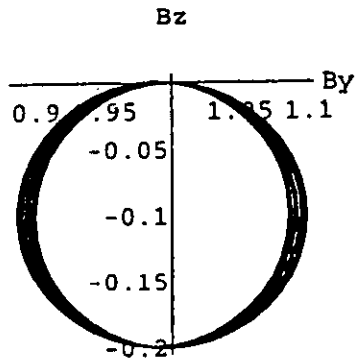
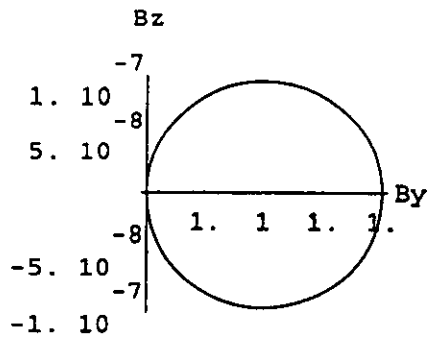
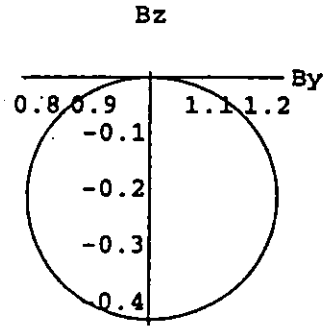


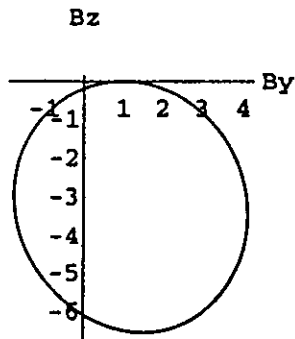
Fig. 8



a = 0.8



a = 10



a = 25

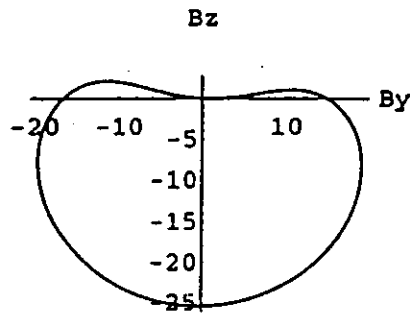


FIG. 9